

Electrical Resistivity of Concrete Made With GGBS as Partial Replacement of Cement

¹Mahmud, Abba Tahir

Department of Building Technology
Federal Polytechnic Bauchi, Nigeria.
abbatm2006@yahoo.com

²Ya'u Jamilu

Department of Building Technology
Abubakar Tafawa Balewa University
Bauchi, Nigeria.
yaumsc3748@gmail.com

³Yusuf, Mohammed Nura

Department of Building Technology
Federal Polytechnic Bauchi, Nigeria.
danyusufanbakori@gmail.com

⁴Ibrahim Idris

Department of Building Technology
Federal Polytechnic Bauchi, Nigeria.
iimatinja@yahoo.com

⁵Muhammad, Nura Isa

Department of Building Technology
Abubakar Tafawa Balewa University
Bauchi, Nigeria.
Mni211@yahoo.com

Abstract—This study is aimed at assessing the electrical resistivity of concrete made with ground granulated blast furnace slag (GGBS) as partial replacement of cement, a two point embedded multi-electrode array system was used to obtain the resistivity at discrete depths within the cover zone of the concrete. A total number of four concrete specimen of 250mm x 250mm x 150mm ordinary Portland cement concrete and ordinary Portland cement replaced by 65% ground granulated blast furnace slag (GGBS) with water/binder ratios of 0.35 and 0.65 were produced and cured for 28days. The data was collected and analysed. Results obtained shows that the addition of GGBS changed the pore structure of the concrete which resulted in higher resistivity. Also, the specimen with w/b ratio of 0.35 showed higher resistivity at all depths irrespective of GGBS. It was concluded that GGBS concrete exhibited higher resistivity than the control samples and as such it is prone to higher rate of deterioration. It was recommended among others that, lower percentage of GGBS replacement of OPC could yield higher performance of concrete.

Keywords—GGBS, Concrete, durability, Electrical resistivity, Electrical measurement

I. INTRODUCTION

Concrete, as a building material, is subjected to a variety of environments, which affects its durability in a variety of ways. A key cause for concrete degradation is as a result of corrosion of steel reinforcement. The cover zone of the reinforced concrete which provides protection to steel is exposed to physical actions such as freeze thaw attack and weathering and chemical actions such as chloride ingress. Equally, when exposed, concrete is affected by transport properties such as absorption, permeability and diffusion and when that happens

through the cover zone of the concrete, the steel reinforcement will corrode. Subsequently, the concrete cracks as a result of the increased stresses which occur on the surface of the reinforcement.

Electrical resistivity is a good non-destructive test for evaluating the concrete durability. The electrical properties behave similarly in movement through the concrete with transport properties such as absorption, permeability and diffusion move through the concrete. The durability of concrete can be predicted if the electrical resistivity is known because it indicates the ease of flow of the different transportation properties.

The premature deterioration of concrete structures is a world-wide problem. In most developed countries, including the UK, around 50% of the construction budget is devoted to repair and maintenance of structures around 30% of this expenditure on concrete structures [2].

The development of integrated monitoring systems for new reinforced concrete structures could also reduce costs by allowing a more rational approach to the assessment of repair options; and, co-ordination and scheduling of inspection and maintenance programmes. The development of sensors and associated monitoring systems to assess covercrete performance would thus form an important element in the inspection, assessment and management of structures [4] in [2]. At present, very little in-situ monitoring of the deterioration of concrete structures is undertaken, primarily due to the lack of reliable methods that provide the information that will allow estimation of residual life. To this end, this paper highlights developments in the use a multi-electrode array embedded within the covercrete to facilitate real-time monitoring of both the spatial distribution and temporal changes in electrical conductivity (and temperature), herein after called the sensor. The electrical properties of concrete are directly related to those properties of concrete which promote the ingress of water and water containing deleterious ionic

species, furthermore, once passivity has been lost, the electrical conductivity of the concrete surrounding the steel reinforcement plays an important role in corrosion dynamics ([5], [6] and [7]) in [2]. It is understandable that a knowledge of the protective properties of the cover-zone is crucial in attempting to make predictions as to the in-service performance of the structure with regard to likely deterioration rates for a particular exposure condition and compliance with specified design life. Regarding cover-zone properties, it is transport processes which are important and terms such as diffusivity (both moisture and ionic), permeability and sorptivity are used in this respect. There clearly exists a need to study and determine quantitatively those near-surface characteristics of concrete which promote the ingress of gases or liquids containing dissolved contaminants and defining concrete performance in terms of a *durability parameter* [1].

II. MATERIAL, SAMPLE AND CURING

The sample comprised of OPC clinker combined with ground granulated blast furnace slag as Supplementary Cementitious Materials (SCM) used in blending was combined in accordance with BS EN 197-1:2000. A water binder ratio of 0.35 and 0.65 were used. The sand used was concreting sand with a maximum particle size of 4mm along with two grades of crushed granite (10mm and 20mm) of low porosity (~0.7%-0.9%). Plasticizer polycarboxylate SikaPlast, conforming to [3]. Specimens were 250x250x150mm (thick) slabs, the upper surface of each slab had a 20mm high ponding area which held water, hence, allowing water to be ponded on the surface of the slab.

III. EXPERIMENTAL AND TEST PROCEDURE

A. Two point multi-electrode array set-up

This experiment used a two point embedded multi-electrode array system. The set-up of the inverted T shaped PVC which holds the electrode in place is illustrated in Figure 3.1. Each electrode was made up of stainless steel pins of 1.6mm diameter. A stainless steel of 10mm diameter was exposed on the end of each electrode. The electrodes were spaced horizontally at 10mm interval, and then vertically spaced at depths of 10mm, 20mm, 30mm, 40mm, 50mm, and 75mm respectively from the surface of the specimen. In order to ensure better distribution around the probes when pouring, the electrodes were overlapped against each other in a vertical plane. The tip of each probe exposed was placed at a distance of 45mm from the face of the T shaped PVC so as to reduce the aggregate-wall-effect. In order to take temperature readings during the experiment, thermistors were integrated into the face of the PVC former at varying depths of 10mm, 30mm, 50mm and 75mm. the data collected were then corrected to temperature. The thermistor resistances were then converted to temperature readings in (^oC) and kelvin (K) using the Stein-Hart equation:

$$T = [A + B \ln R + C (\ln R)^3]^{-1} - 273.15 \dots \text{Equation 3.1}$$

$$T = [A + B \ln R + C (\ln R)^3]^{-1} \dots \dots \dots \text{Equation 3.2}$$

Where,

R = the measured resistance of the thermistor (ohms)
 T = temperature (^oC) and K;

A, B, C = coefficients which depend on the type of thermistor, were calculated from manufacturer data, respectively, to be: 1.287600011x10⁻³ K⁻¹; 2.357183092x10⁻⁴ K⁻¹ and 9.509464377x10⁻⁸ K⁻¹.

Ln = natural logarithm.

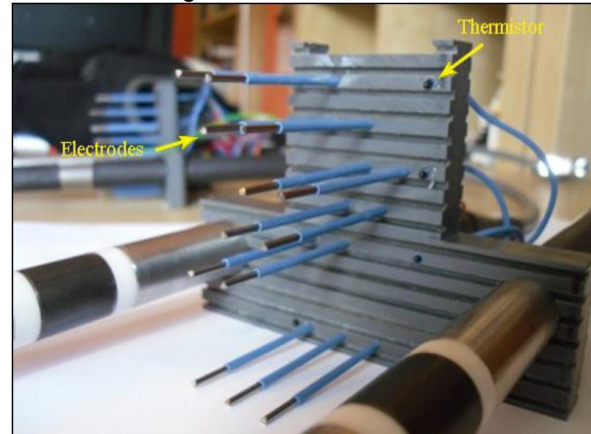


Figure 1: Multi Electrode sensor array

B. Electrical Measurement System

An automated measurement system was used to gather two-point resistance data from the electrode embedded array system in the concrete slabs. The system consists of a concrete resistance logger linked to a multiplexing unit, which allows up to seventy two 2-point channels to be monitored via six 37-way D-type connector and cable assemblies. Measurements are obtained using a 1000 mV peak to peak ac voltage signal (350 mV rms) at 1000 Hz. The logger stores measured resistance data in an operator pre-programmed format to a non-volatile memory. As-measured data is uploaded in 39 Microsoft Excel csv format for subsequent processing to a personal computer (PC) via an RS232 port connector. The logger was set to record a cycle reading at every 5minutes interval for a period of 24 hours.

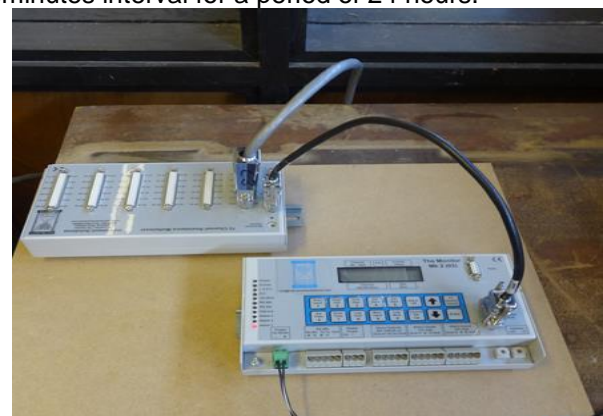


Figure 2: Measurement system

IV. RESULT AND DISCUSSION

In order to study the varying effects of the w/b ratio and the direct influence of GGBS additive, an analysis was conducted on the data obtained from the specimens with w/b ratios of 0.35 and 0.65. The resistance from the logger was used for the analysis without any correction. Graphs were plotted for the resistance (ohms) versus corrected temperature ($^{\circ}\text{C}$) for each specimen at varying depths of 10mm, 30mm, 50mm and 75mm respectively, containing the various w/b ratios mentioned above. Concrete with low resistivity signifies that the current can flow easily through the concrete material. Nevertheless, resistivity in concrete is related with how interrelated the voids are, the amount of ions present and also the degree of saturation.

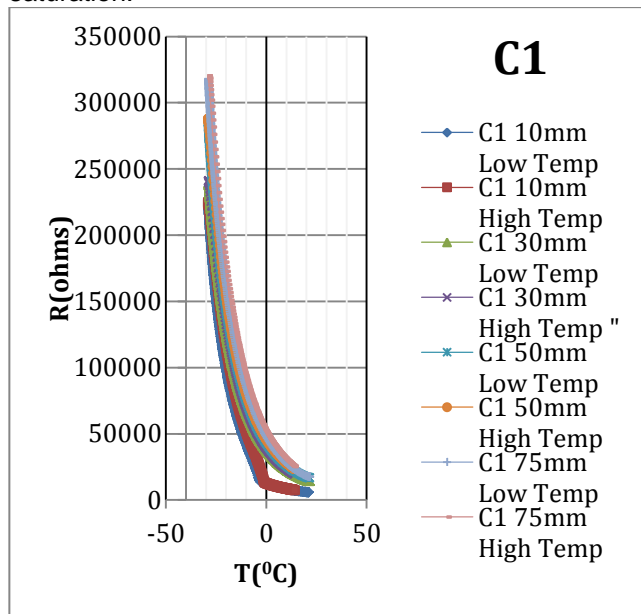


Figure 3: Resistivity vs. Temperature for specimen C1

Specimen C1 (100% OPC and 0.35 w/b ratio) is presented in Figure 3. The electrical resistivity increases with depth of concrete cover. The lowest resistivity is observed at depth 10mm and increased with depth. This could be that the ice propagates gradually with depth from the surface of the specimen. Hence, as the temperature increases, the resistivity decreases with the depth. The electrical resistivity increases slightly but then rapidly at a temperature below 0°C to about -3°C . This could be attributed to crystallization of the pore water at lower temperature and liquidization as the temperature increases. The decrease in resistivity is observed to be rapid but then slightly at temperature of about -1°C and it is accompanied by increase in the temperature. It is quite interesting to know that the resistivity varied smoothly and similarly at depths of 30mm, 50mm and 75mm. However, with the resistivity increasing slightly in the order of depth 30mm, 50mm and 75mm respectively, it is reasonable to assume that at lower depths, the permeability of the pore system decreases which in turn increases the resistivity. However, the exact opposite action takes place at higher temperature.

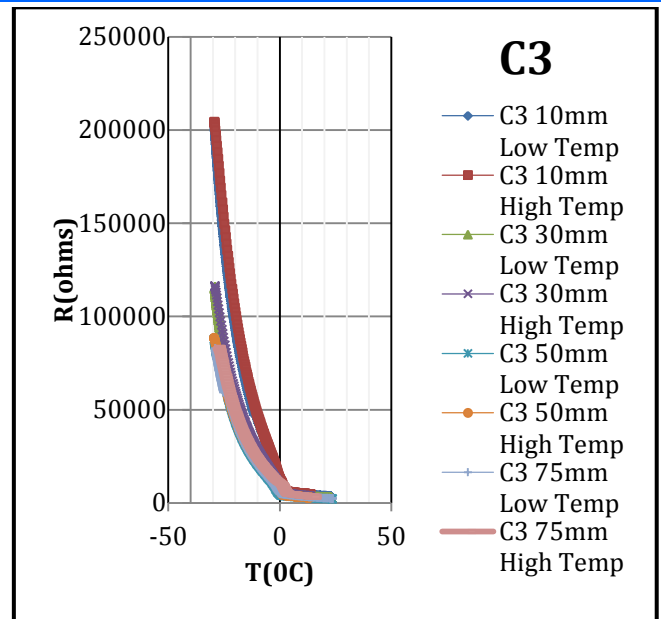


Figure 4: Resistivity vs. Temperature for specimen C3

In analysing specimen C3 (100% OPC and 0.65 w/b ratio), it can be observed that a similar action takes place to that seen in specimen C1 at depth 10mm. However, the resistivity is much lower than that of specimen C1. The electrical resistivity decreases with depth. The resistivity at depth 10mm is higher compared with depths 30mm, 50mm and 75mm respectively. The action is opposite to C1 which increases with depth. Hence, the decrease in resistivity could be that the specimen is less permeable at the upper surface and thus ice formation takes place at the upper surface. The resistivity increases slightly as temperature approaches 0°C and then rapidly as temperature further decrease, which is the case at all depths. However, at higher temperature, the action is opposite. The resistivity decreases as the temperature increases. The decrease is abrupt but then slightly as temperature reaches about 2°C .

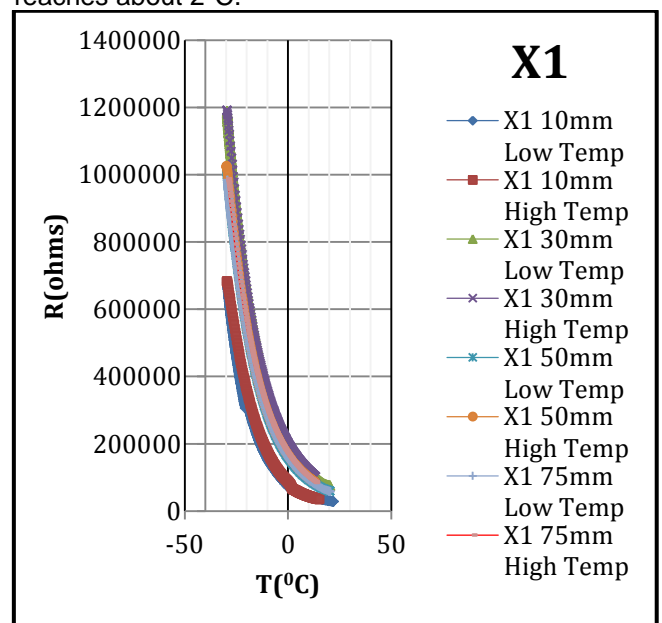


Figure 5: Resistivity vs. Temperature for specimen X1

In analysing specimen X1 (65% GGBS and 0.35 w/b ratio), it can be seen that increase in resistivity is as a result of decrease in temperature. The increase can be observed to be abrupt in the region of sub-zero temperature. The resistivity varied smoothly and similarly at depths of 10mm, 30mm, 50mm and 75mm above and below 0°C which could indicate that the phase transition did not affect the resistivity. The resistivity is lower at depth of 10mm but then increased sharply at depth of 30mm and then slightly decreased at 50mm and 75mm respectively. This could be that as ice percolates through the pores down, less effect is being observed, but the effect is more at depth 30mm due to higher resistivity. However, the exact opposite action takes place at higher temperature. The decrease in resistivity as observed is associated with increase in temperature.

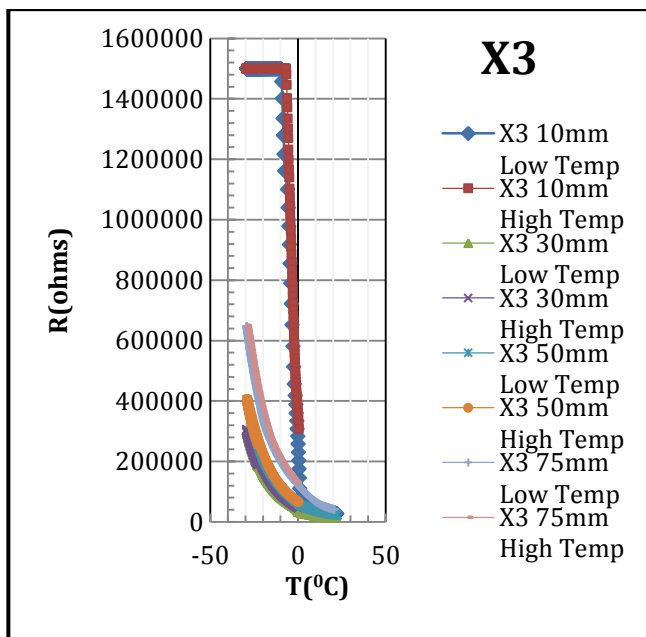


Figure 6: Resistivity vs. Temperature for specimen X3

In analysing specimen X3 (65% GGBS and 0.65 w/b ratio), it can be seen that resistivity at depth 10mm increases gradually as temperature decreases and approaches 0°C, but then another sudden change occurs at much lower temperature of about 10°C. The resistivity remains constant as that is the maximum resistivity in the measurement logger. The decrease in resistivity is accompanied by the increase in temperature. As the temperature changes, it can be observed that the resistivity remains constant until it reaches a temperature of about -6°C but the rapidly decreases when it reaches a temperature of about 2°C, another sudden change takes place. This again could be attributed to varying pore sizes within the pore system melting at different temperatures. The sudden or abrupt increase in resistivity between 2°C and about -10°C could be due to ice formation at surface of the specimen. It is also logical to think that the resistivity increases at lower temperature as most of the pores freezes at a much lower temperature. At

depths of 30mm, 50mm and 75mm, the resistivity is lower

V. CONCLUSION

In comparing the resistivity of the various samples (X1, X3, C1 and C3), it can be observed that the largest values of resistivity were shown by concrete specimens with low water/ binder ratio (w/b ratio= 0.35) irrespective of addition of GGBS. This may be attributed to lower porosity due to the amount of water used. Equally as mentioned previously in literature, high resistivity indicates low permeability. It is worth nothing that the addition of GGBS which produced a refinement in the pore structure possibly results in higher resistivity irrespective of water/binder ratio. The electrical resistivity of all specimens increased with decrease in temperature and decreases with increase in temperature. Because the concrete specimens freezes at higher temperature and melts at lower temperature at the surface 10mm depth, measures should be taken to provide protection at the surface to avoid ice propagating to the rebars.

REFERENCES

- [1] McCarter, W., Chrisp, T., Starrs, G., Owens, E., Holmes, N., Basheer, L., Nanukuttan, S., Basheer, M.: Conductivity Sensors to Monitor Cover-Zone Performance. Concrete in Aggressive Aqueous Environments. Toulouse, France, 2009.
- [2] McCarter, W., Chrisp, T., Starrs, G., Holmes, N., Basheer, L., Basheer, M., Nanukuttan, S.: Developments in Monitoring Techniques for Durability Assessment of Cover-Zone Concrete. 2nd International Conference on Durability of Concrete Structures, Sapporo, Japan, November, 2010.
- [3] European Committee for Standardization (CEN), EN 197-1: 2000, 'Cement – Part 1: Composition, specifications and conformity criteria for common cements', Brussels.
- [4] Buenfeld, N. R., Davies, R., Karimi, A and Gilbertson, A., 'Intelligent Monitoring of Concrete Structures', CIRIA Report (C661), Jan. 2008, ISBN 978-0-86017-661-9.
- [5] Broomfield, J. P., 'Corrosion of steel in concrete', E&FN Spon, London, 1997, 240pp, (ISBN 0419 19630 7).
- [6] European Union – Brite EuRam III, 'Duracrete – Modelling of degradation', Report BE95-1347/R4-5, 1998, Dec., 174pp, (ISBN 90 376 0444 7).
- [7] European Union – Brite EuRam III, 'Duracrete – Models for environmental actions on concrete structures' Report BE95-1347/R3, 1999, Mar., 273pp, (ISBN 90 376 0400 5).